Journal of the Brazilian Society of Mechanical Sciences and Engineering (2020) 42:348
https://doi.org/10.1007/s40430-020-02422-2

TECHNICAL PAPER

Investigation of the effect of surface crack on low-velocity impact response in hybrid laminated composite plates

Aydın Güneş[1] · **Ömer Sinan Şahin**[2]

Received: 31 October 2019 / Accepted: 15 May 2020 / Published online: 4 June 2020

Abstract

Composite materials can be damaged in the environments in which they are used, due to the loads they are exposed to or due to different effects on the production processes. The formation processes of these damages generally develop as crack formation or progress of the existing crack. For this reason, it is very important to investigate the behavior of the crack that occurs after the dynamic loads to which the composite materials are exposed. In this study, the dynamic behaviors of hybrid laminated composites with different surface crack geometries were investigated. Surface cracks with different crack depth-to-thickness (a/t) and crack depth-to-crack width (a/c) ratios were machined upon hybrid composite laminates and subjected to low-velocity impact tests under 2 m/s, 2.5 m/s and 3 m/s impact velocities. The effect of different surface crack geometries upon variation of contact force versus time, variation of contact force versus displacement and variation of absorbed/rebound energy have been evaluated. The effect of surface crack geometry and impact velocity upon contact stiffness and bending stiffness was also evaluated. Damage formation during impact loading was examined by scanning electron microscopy and optical microscopy. After the evaluations, the damage behaviors caused by the dynamic loads depending on the initial surface crack geometry were examined in detail.

Keywords Low-velocity impact · Hybrid laminated composite · Surface crack · Dynamic response · Delamination

1 Introduction

Nowadays, the application areas of composite materials are increasing rapidly. Many areas such as aviation, automotive and defense industry continue to work to obtain composite materials with better properties [1]. Composite materials may be subject to dynamic loads during production or their use, depending on working conditions which may result in unexpected damage.

Epoxy resins with their excellent physical and chemical properties are considered essential for so many engineering applications [2]. Owing to their advantages, carbon fiber-reinforced polymer composites have been widely utilized in aerospace, automobile and defense industries [3, 4]. Polymer materials are generally ductile in semi-static load depending on the type. However, the stiffness and strength of material increase at relatively high strain rates [5].

Hybridization and stacking sequence are very important and essential for the design of composite materials. Some researchers have focused on this topic [6–23]. Hosur et al. [10] have focused on low-velocity impact response of woven glass and woven carbon-reinforced composite plates. They also investigated the damage formation and progression. Sevkat et al. [14] have performed a drop weight test on glass–graphite/epoxy hybrid composites and compared the experimental results with finite element analyses.

The formation and progression of surface cracks are also very important in composite materials [1, 24, 25]. For this reason, materials are expected to exhibit the mechanical behavior predicted in the design and keep the structural integrity under impact loads [26–28]. The chemical and mechanical effects on the surface of materials may result in notches or cracks [29]. The useful life of composite materials can be affected because of these effects. Even a small impact can result in a large effect [24, 25]. The internal damage that is not visible to the naked eye in composite materials is the general characteristic of the composite material.

✉ Aydın Güneş
aydingns@hotmail.com

[1] Department of Mechanical Engineering, Abdullah Gül University, 38080 Kayseri, Turkey

[2] Department of Mechanical Engineering, Konya Technical University, 42075 Konya, Turkey

The damage on the materials starts in this way causing the strength and rigidity of the composite materials to decrease, and this effect becomes even greater under relatively higher loads [25, 30–34]. Also, damage formation can take place on the back surface of the impacted object. Impact loading can also result in internal delamination between layers [35–37]. Although the impact response in the metals is in the form of a break or break as a result of the plastic deformation, the composite materials can be damaged in many different modes [25, 38] such as matrix cracking, debonding, delamination and fiber breakage.

Many studies have been carried out on the mechanical behaviors of composite materials with surface cracks exposed to different loading conditions. In these studies, the mechanical properties of the composite materials with surface cracks were compared with the composite materials without surface cracks [39–47]. The effect of the surface crack on the mechanical properties of composite materials was evaluated regarding the parameters such as the energy dissipation rate (J), the stress intensity factor (K) and the position of the crack. Both experimental and numerical analyses of composite materials made of aluminum and polymer materials (PMMA) were carried out under dynamic loads [48, 49].

The literature review revealed that the mechanical and dynamic responses of composite materials subjected to impact loading had extensively been investigated. However, no study has been found which focuses on the dynamic response of composite laminates with a surface crack. Therefore, this study will make an important contribution to the literature.

This study aims to investigate the dynamic response of laminated composite plates with a surface crack. For this aim, surface cracks with different shapes and sizes have been machined on hybrid laminated composites and subjected to low-velocity impact at different speeds. The variation of contact force versus time, the variation of contact force versus displacement and the variation of energy concerning time were examined experimentally. Damage formation during impact loading was also evaluated by Scanning Electron Microscopy (SEM) and optical microscopy. The results were evaluated under separate titles, and the effects of different surface crack geometries on the impact behavior of laminated composite materials were examined at length.

2 Experimental study

2.1 Materials

The epoxy (Hexion-EPR840-EPH875) resin was used as matrix material in the production of composite materials, while carbon fiber and glass fiber were used as reinforcing material. Although glass fibers are mainly used in the production of composite materials, supportive carbon fibers are used in the middle layer to increase rigidity. The mechanical properties of the constituents used in production are shown in Table 1. In Table 1, E_1 and E_2 represent the modulus of elasticity in fiber direction and transverse direction.

Hybrid laminated composite materials were produced by a hot-pressing method with curing at 120 °C for 4 h and then cut at the specified dimensions; these processes were carried out by IZOREEL Company (Izmir/Turkey). Hybrid laminated composites used in our experimental study have 18 layers and a geometry having dimensions of 90 mm × 25 mm × 4 mm. The middle two layers of the 18 layers came from the carbon fiber layers and the other layers from the glass fiber layers as shown in Fig. 1. The carbon fibers used in the middle layer are used to increase bending stiffness and are not affected by initial crack geometries.

The parameters determined for the experimental studies are shown in Table 2. The surface cracks were machined on the surface of the hybrid layered composite materials by using carbon disks. To achieve the desired values of crack depth (a) and crack width (c), a tool sharpening bench was used to reduce the diameter to the determined value. After that, the carbon disk tool was connected to the tool grinding machine and machined to the desired diameter. The surface notches were then machined with the help of the milling machine. After that, the machined surface notches have been sharpened by using lancet to convert them into surface cracks.

According to classical lamination theory, the bending stiffness of a composite plate is directly related to the position of layers concerning middle plane and stiffness of every single ply. It is aimed to increase the bending stiffness by positioning the carbon layer in the middle part [25, 39]. The strength and moment values of each layer can be collected to obtain the strength and moment values of the layered composite. Force and moment statements can also be obtained in matrix form [27]:

Table 1 Properties of composite constituents

Properties of constituents	
Carbon fiber	Glass fiber
$E_{carbon} = 230$ GPa	$E_{glass} = 72$ GPa
Properties of carbon/epoxy and glass/epoxy plies	
Carbon/epoxy ply	Glass/epoxy ply
$E_1 = 136.93$ GPa	$E_1 = 47.16$ GPa
$E_2 = 7.18$ GPa	$E_2 = 7.76$ GPa
Tensile strength = 4 GPa	Tensile strength = 2.4 GPa
Poisson's ratio $\nu_{12} = 0.30$	Poisson's ratio $\nu_{12} = 0.27$
Density = 3.6 gr/cm^3	Density = 2.5 gr/cm^3

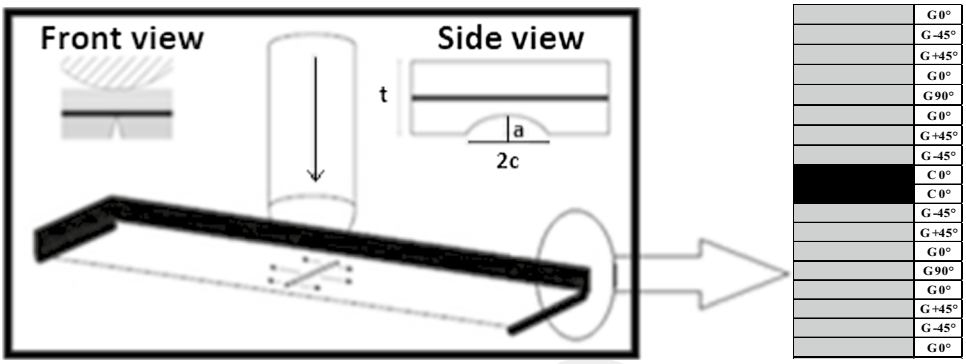

Fig. 1 The stacking sequence of hybrid laminated composite and surface crack

Table 2 Geometric parameters of surface cracks and specimen numbering

Specimen number	*a/c*	*a/t*	*t* (mm)
1	0.3	0.5	4
2		0.45	
3		0.4	
4		0.35	
5		0.3	
6		0.25	
7	0.4	0.5	
8		0.45	
9		0.4	
10		0.35	
11		0.3	
12		0.25	

$$A_{ij} = \sum_{k=1}^{N} \left(\bar{Q}_{ij}\right)_k \left(z_k - z_{k-1}\right)$$
$$B_{ij} = \frac{1}{2} \sum_{k=1}^{N} \left(\bar{Q}_{ij}\right)_k \left(z_k^2 - z_{k-1}^2\right) \quad (1)$$
$$C_{ij} = \frac{1}{3} \sum_{k=1}^{N} \left(\bar{Q}_{ij}\right)_k \left(z_k^3 - z_{k-1}^3\right)$$

$$\left(\bar{Q}_{11}\right)_k = \frac{E_1^k}{1 - V_{12}^k V_{21}^k}, \left(\bar{Q}_{12}\right)_k = \frac{v_{12}^k E_1^k}{1 - V_{12}^k V_{21}^k},$$
$$\left(\bar{Q}_{22}\right)_k = \frac{E_2^k}{1 - V_{12}^k V_{21}^k}$$
$$\left(\bar{Q}_{16}\right)_k = 0, \left(\bar{Q}_{26}\right)_k = 0, \left(\bar{Q}_{66}\right)_k = G_{12}^k \quad (2)$$

In these formulations, A_{ij} represents the extensional stiffness coefficient, B_{ij} represents the bending-extension coupling stiffness coefficient, and D_{ij} represents the bending stiffness coefficient. Because laminated composite materials were symmetrical, B_{ij} was considered to be zero in this solution. Using the E_1 and E_2 values in Table 1, the calculation of the above statements for each layered composite material yielded a single stiffness matrix for the entire layered composite material. Table 3 shows the elastic constants for tested laminated composite material. The fact that the D_{11} matrix shown in Table 3 is considerably higher than the others shows the advantage of carbon fiber positioning in the middle of the laminate's arrangement in bending stiffness.

2.2 Impact tests

The hybrid laminated composites with surface crack have been subjected to low-velocity impact tests by using a drop tower by varying the height of the dropping impactor. The impactor has a mass of 5.6 kg and a hemispherical tip with a diameter of 12 mm. The testing machine and impactor are supposed to be perfectly rigid. The force signals were measured by a sensor in the millivolts scale. The signals were first amplified by a signal processor and transmitted to the data acquisition card. The variations of the interaction force between the impactor and the sample versus time were obtained by using NI Signal Express software. The sampling rate of the data acquisition system is 25 kHz. As described in the ASTM-D7136 standard, Newton's second law of motion was used to express the velocity and displacement of impactor versus time. With the first integration of accelerations as a function of time, the velocity and, with the second integration operation, displacement values achieved.

When the impactor first hits the simply supported material, the kinetic energy of the impactor is partly transferred to the material. The remaining kinetic energy is used for rebound which makes the impactor to rise. This process continues until the kinetic energy of the impactor is fully consumed. During this process, the material is generally subjected to 12–15 impacts. The testing machine has an anti-rebound system which allows us to get only one impact. Figure 2 shows the low-velocity impact test machine [1].

Table 3 Stiffness values of laminated composite materials

A_{ij}: Extensional stiffness coefficient					
A_{11}	A_{12}	A_{22}	A_{16}	A_{26}	A_{66}
695.9	118.2	273	81.1	81	101.9
B_{ij}: Bending-extension coupling stiffness coefficient					
B_{11}	B_{12}	B_{22}	B_{16}	B_{26}	B_{66}
0	0	0	0	0	0
D_{ij}: Bending stiffness coefficient					
D_{11}	D_{12}	D_{22}	D_{16}	D_{26}	D_{66}
14530.5	3133.4	6802	2170.8	2168.2	2726.5

3 Results and discussion

3.1 Effect of surface crack parameters

3.1.1 Variation of force versus time

Figures 3 and 4 show the effect of varying *a*/*t* values on the force–time behavior of the material under three different impact velocities when *a*/*c* is constant. Fluctuations observed in force–time curves are reported to be the indication of matrix damage [50, 51]. The damage initiation is generally characterized by a dropped first force value suddenly. While matrix damage generally causes small fluctuations in the force–time curve, debonding or fiber breakage leads to significant decreases in force values. In addition, heavy damage such as delamination leads to a significant change in the slope of force–displacement curves. It is observed in Fig. 3 that when the *a*/*c* ratio is constant, the maximum force value decreases as the surface crack deepens. On the other hand, it is observed that higher impact velocities result in larger interaction times. The interaction time has two components. The first is the elastic deformation, and the second is the time required for permanent damage. The time required for the formation and return of elastic shape change is the same. However, permanent damage is required for a certain period. The increased interaction time indicates that damage has occurred. It was observed that the interaction time was affected by the crack width (*c*) at 2 m/s and 2.5 m/s where the impact speed was partially low. Interaction times were generally longer at $a/c = 0.3$ where the crack width was large. However, similar behaviors have been observed in samples where the impact velocity is 3 m/s due to the increase in permanent damage amounts.

The peak force can also be considered as criteria for impact resistance. The size of the damage zone is also affected by the absorbed energy during impact [52]. Fiber breakage [53] and fiber pullout [54], which is an indication of low fiber/matrix adhesion, can take place.

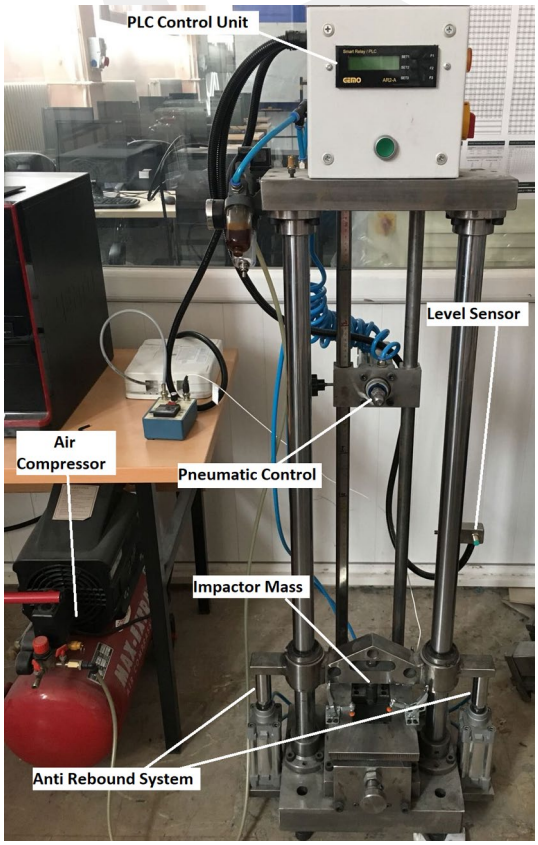

Fig. 2 Low-velocity impact test units

The force–time curves are very smooth when the impact velocity is 2 m/s. However, increasing impact velocity has led to a variation on force–time curves. As seen in these figures, force–time variations for impact velocities 2.5 m/s and 3 m/s show some oscillations which are indication of damage formation and progression. In particular, when impact velocity is 3 m/s, impact force showed sudden decrease which is an indication of severe damage formation such as fiber pullout or fiber breakage. Similar behavior can be

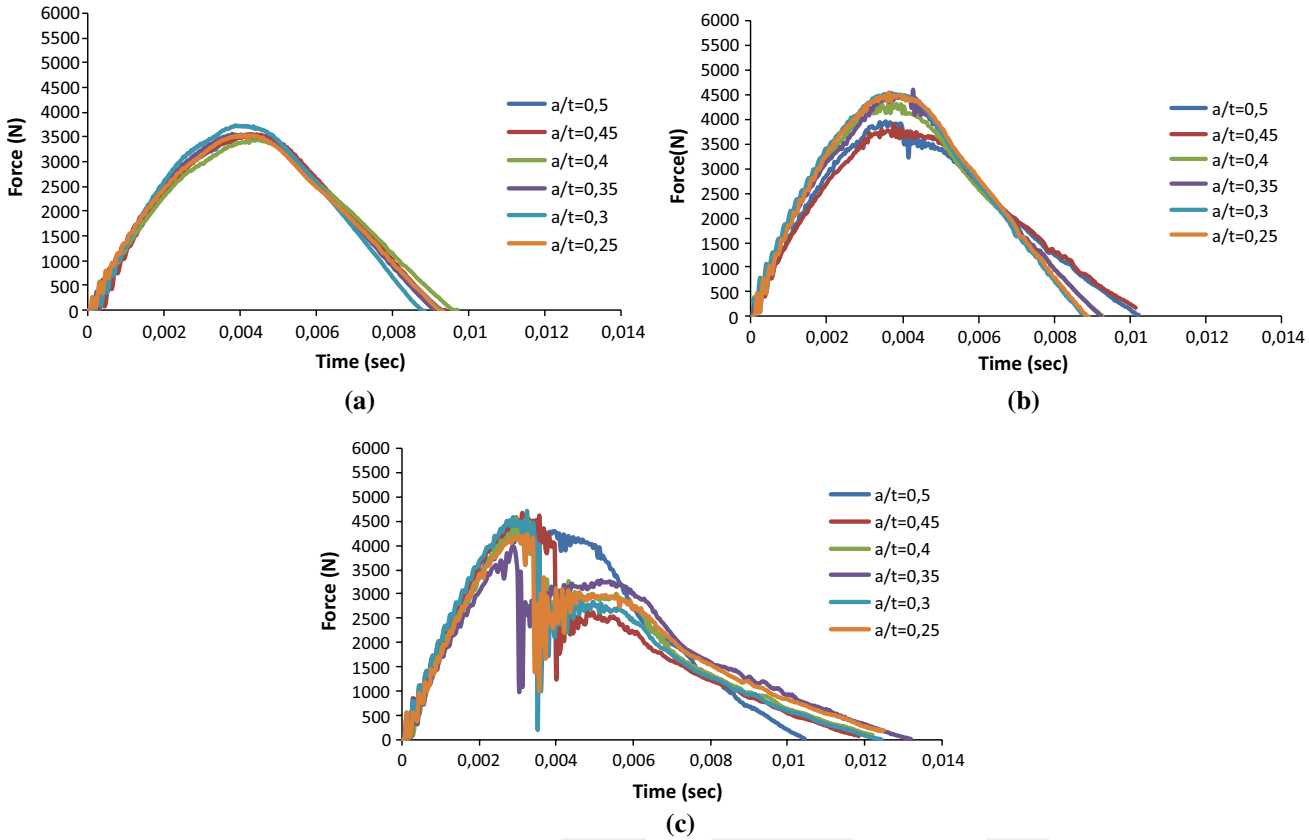

Fig. 3 Effect of different surface crack geometries on force–time behavior ($a/c = 0.3$). **a** 2 m/s, **b** 2.5 m/s, **c** 3 m/s

observed at an impact velocity of 2.5 m/s but on a limited scale. Bending resistance of fiber-reinforced composites is formed by fibers. The sudden decrease in bending resistance occurs when the fibers are broken or debonding the fibers. The sudden decrease in resistance and an increase in the aftermath show that the fibers are formed by the short distance of the debonding. Due to this phenomenon, longitudinal waves form in the fiber direction. This situation shows itself as fluctuations observed in force value [55].

Figures 3c and 4c show the change in force with time at the impact velocity of 3 m/s. The maximum force value changes depending on the crack depth. It is seen that the surface crack geometry is the effective parameter in the development of force over time from the moment the impactor touches the composite surface. The fact that the surface crack is deep or wide affects the stiffness of the composite material significantly. For example, when $a/t = 0.5$ in Fig. 4c, the reduction of the force occurs after about 4100 N, whereas when the ratio $a/t = 0.25$, decrease of about 4600 N occurs. This concerns the geometry of the surface cracks created in the specimens. As the depth of the surface cracks increases, the number of cut layers during machining of surface cracks increases and the sample resistance is adversely affected.

The contact force starts to increase with just first contact and continues until the Hertzian failure is encountered. The Hertzian damage can be associated with the matrix cracking failure encountered in the contact region. However, the composites did not lose their structural integrity and that can show resistance against the applied deformation thanks to the stiffness provided by the fiber reinforced.

Table 4 shows the values of maximum and critical forces. The force–time histories of all impact tests have been examined to evaluate the relationships between P_{cr}, P_m and time with the impact energy. The critical force, P_{cr}, represents the force for which the first considerable decrease occurs. This decrease is caused by the degradation of the transverse stiffness of the laminate. The maximum force, P_m, represents the maximum force reached, and P_r shows the resistance strength value reached after damage [55].

In Table 4, values $a/t = 0.25$–0.35 can be considered as shallow crack, $a/t = 0.4$ and above values as deep crack. With the decrease in a/t values, the surface crack becomes shallower. In this case, P_{cr} is regularly increasing. This is an expected result. Deep and shallow surface cracked specimens behave differently as the impact velocity increases because of absorbed energies change. But in general, the P_m increases with increasing impact velocity. This situation

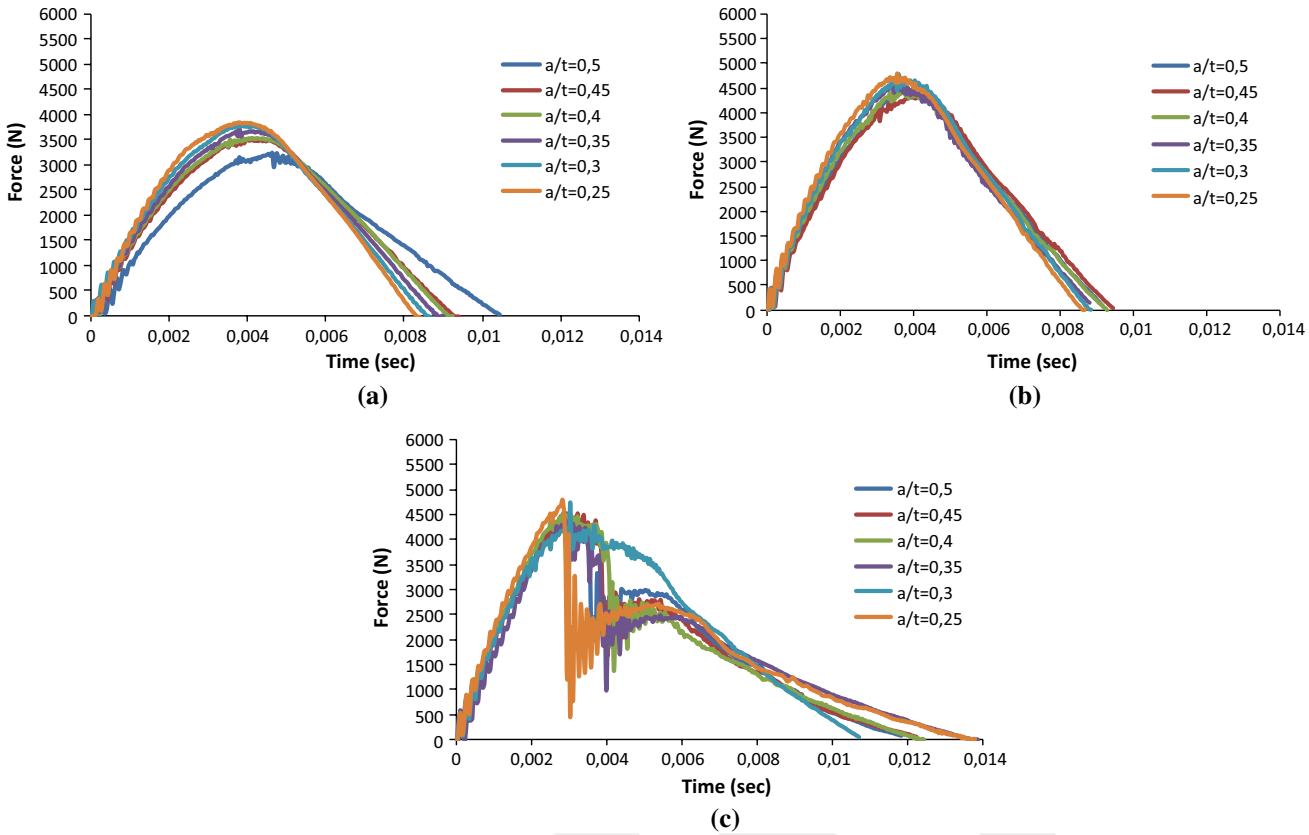

Fig. 4 Effect of different surface crack geometries on force–time behavior ($a/c = 0.4$). **a** 2 m/s, **b** 2.5 m/s, **c** 3 m/s

Table 4 Values of maximum, residual and critical forces

a/c	*a/t*	2 m/s			2.5 m/s			3 m/s		
		P_m (N)	P_{cr} (N)	P_r (N)	P_m (N)	P_{cr} (N)	P_r (N)	P_m (N)	P_{cr} (N)	P_r (N)
0.3	0.5	3450.14	N/A	N/A	3892.39	3696.12	3363.11	4474.64	4074.35	3303.56
	0.45	3461.53	N/A	N/A	3898.12	3723.65	3592.92	4518.8	3933.58	1156.84
	0.4	3475.19	N/A	N/A	4382.26	4116.34	4004.26	4384.2	3854.81	1195.14
	0.35	3477.92	N/A	N/A	4407.42	4242.66	4074.33	4081.6	3903.92	1017.22
	0.3	3521.17	N/A	N/A	4421.17	N/A	N/A	4520.88	4068.47	496.51
	0.25	3528.06	N/A	N/A	4457.38	N/A	N/A	4270.79	3952.22	1008.35
0.4	0.5	3363.34	3344.53	3321.2	4393.22	4103.9	4056.87	4290.44	3914.55	2151.4
	0.45	3639.27	3341.66	3297.69	4371.13	4085.65	4017.92	4489.31	4083.44	2285.08
	0.4	3572.41	3302.84	3272.34	4451.81	4264.72	4086.5	4501.24	4008.3	1351.06
	0.35	3753.44	3545.62	3495.36	4604.85	4509.33	4362.34	4518.43	4206.74	1186.29
	0.3	3825.78	3498.37	3401.52	4696.67	4615.81	4463.29	4691.11	4398.93	3608.25
	0.25	3845.25	3522.08	3467.88	4718.92	4630.56	4516.77	4732.49	4732.49	492.67

varies depending on the width or depth of surface crack in composite materials. Higher P_m values were obtained in samples with low crack width ($a/c = 0.4$).

P_r regularly increases at speeds of 2–2.5 m/s. In other words, as the surface crack becomes shallow, the force value at which the resistance begins to rise again is shifted upward. However, irregular changes are observed at 3 m/s. It is thought that the deformation caused by impact occurs as wave motion and is caused by waves reflected from these regions. Also, the friction force between the laminates is the dominant parameter in the recovery of resistance. In the initial stages of the damage, the bending resistance rebuilds depending on ensuring that the laminates move together again with the friction bond. Due to the fluctuation of the

contact force, the frictional force between the laminates may vary. In addition, when a force exceeds the frictional force between the laminates, situations such as delamination or fiber buckling may occur. This explains the fluctuation of the P_r value as a/t values change.

3.1.2 Variation of force versus displacement

The initial slope of the force–time curve represents the contact stiffness [52], and the initial slope of force–displacement curves represents the stiffness under impact loading [50, 51, 54–59]. In materials, the displacement that occurs after the impact loading and the time reached when the force reaches the maximum are related to rigidity of materials [60–62]. The steeper slopes indicate a more rigid structure. Interlaminar and intra-laminar adhesive properties play an important role in the characteristics of the curve, and consequently, steeper slope also indicates a better interfacial interaction.

The sharp force drops states damage formation in the sample such as fiber pullouts, delamination [60] and a significant reduction in bending stiffness of laminate [63]. Longer contact duration in samples in each impact velocity level implies more damage propagation due to less crack arrest [64]. So it can be concluded that less damage formation is expected in a composite having higher rebound energy due to its elastic capacity.

The most important reason for delamination is the bending stiffness difference between successive plies [24, 65–67] with the help of shear stresses as a result of bending [24, 67]. The delaminations formed between successive laminates are also led by a considerable amount of energy absorption [66–68]. The absorbed energy by the composite materials, besides the formation of delamination, can break the structural integrity of the composite materials by causing breakage or stripping of the fibers. These distortions limit the usage of composite materials by reducing their elastic resistance capacity.

Figures 5 and 6 show the variation of contact force versus vertical displacement of test specimens subjected to low -velocity impact test at different speeds (2 m/s, 2.5 m/s and 3 m/s). In these graphs, the effect of a/t value on the force–displacement behavior of the material is shown when a/c value is constant ($a/c = 0.3$ and $a/c = 0.4$). As shown in Figs. 5 and 6, the value of permanent deformation increases with the increasing impact velocity. The initial slope of the contact force–time curve is defined as contact stiffness, while the initial slope of the contact force–displacement curve is defined as bending stiffness. In particular, it is observed that the bending stiffness increases with the shrinkage of crack depth (a) and crack width (c) parameters at high impact velocity, and in addition, composite materials reach higher force values in smaller deformations.

Table 4 shows the stiffness values of composite materials with surface crack tested under different impact velocities. In low-velocity impact experiments, the contact stiffness depends on the geometry and materials properties of impactor with the elastic behavior of the composite materials. Depending on the selected impactor geometry, it can show either a linear or nonlinear character. Since the selected impactor tip geometry is semi-spherical, the contact stiffness is expected to show nonlinear behavior.

On the other hand, due to the structure of the composite materials, the starting point of contact can be different for each test sample. In this regard, minor variations in contact stiffness can be expected as seen in Table 5. Contact and bending stiffness values show an increase with increasing impact velocity. However, when impact velocity is 3 m/s, both kinds of stiffness decrease. This situation can be associated with damage formation as local matrix cracking at earlier stages of contact in which impactor penetration could have resulted in a very narrow area. With the increase in the energy affecting the contact area, the damage mechanisms within the material develop and reduce the rigidity significantly.

The surface crack geometry also influences the elastic behavior of the specimen regarding contact stiffness and bending stiffness. As seen in Figs. 3 and 4, the slope of force–time curves decreases with increasing a/t ratios. These variations are summarized in Table 5. As seen in Table 5, both contact stiffness and bending stiffness values decrease with increasing a/t ratios as expected. This is due to the fact that for a constant a/c ratio, intact portion of the specimen decreases when the a/t ratio increases. In addition, with increasing crack depth (a), the number of laminates and fibers to carry the applied load decreased and as a result, the stiffness of the surface cracked composite material decreased as in Table 5.

3.1.3 Time-dependent energy transfer

The kinetic energy of the impactor is transferred to the material by various stages with different characteristics. Initially, the kinetic energy is absorbed by the elastic deformation and friction by the material. If the impact energy is much more than the resilience of the material, the excess energy will be absorbed as either plastic deformation or damage formation [50]. It is known that damage development occurs as crack formation, crack propagation, delamination and fiber breakage for fiber-reinforced polymer composites [54, 56, 57]. While the amount of absorbed energy is directly related to damage formation, the rebounded energy is related to elastic properties in composite laminates [68–70].

The composite materials are expected to keep structural integrity in the case of an impact loading. Figures 7 and 8

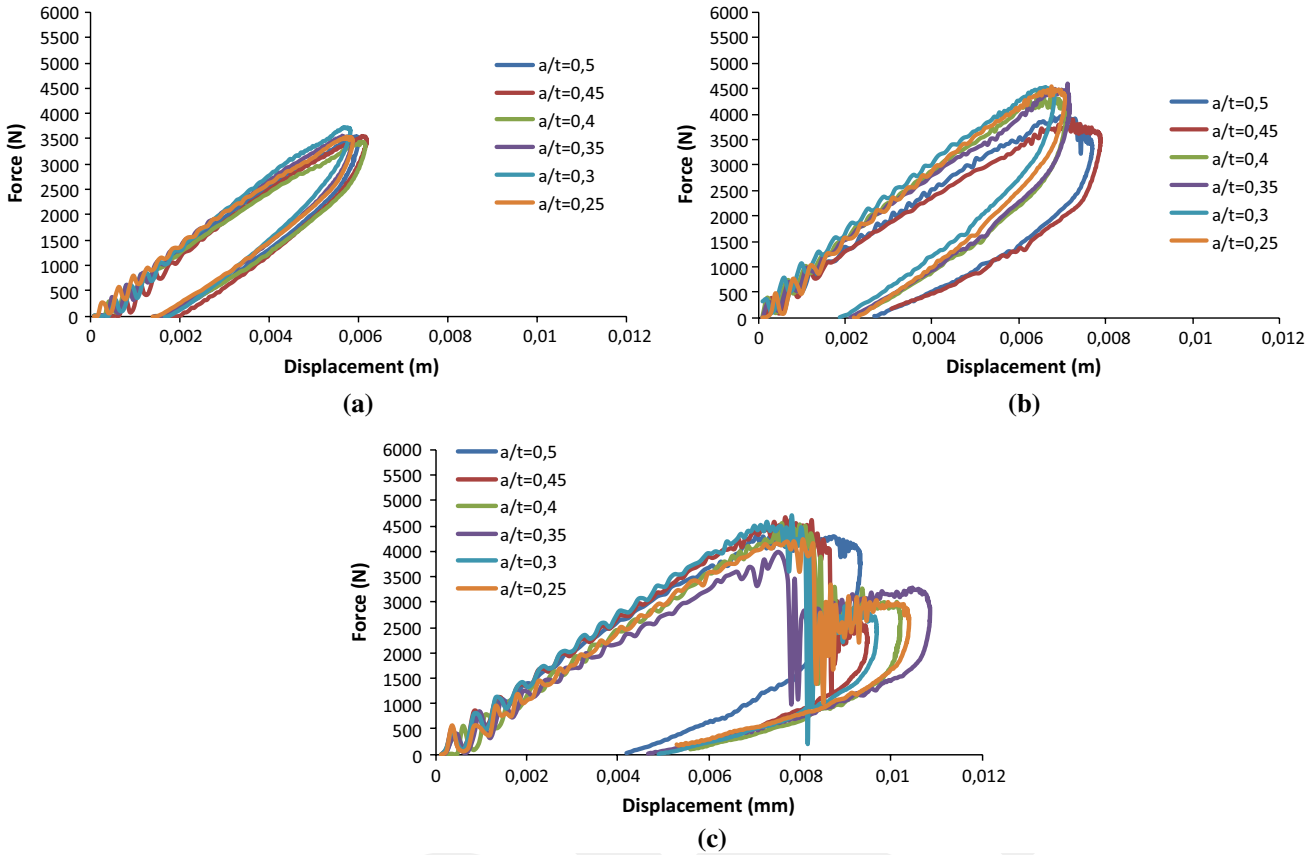

Fig. 5 Effect of different surface crack geometries on force–displacement behavior ($a/c = 0.3$). **a** 2 m/s, **b** 2.5 m/s, **c** 3 m/s

show the energy absorption capacities of the hybrid laminated composites with different surface crack geometries tested under three different impact velocities. The vertical axis shows absorbed-rebounded energies, while the horizontal axis shows test specimens with different a/t ratios.

As can be seen in Figs. 7 and 8, absorbed and rebounded energy levels are close to each other in the tests performed at 2 m/s speed. It is also observed that the effect of the a/t ratio is more pronounced as the impact velocity increases. The amount of absorbed energy decreases with decreasing a/t in specimens when tested under impact velocity of 2.5 m/s. This is because the increase in the ratio a/t causes much more damage development. So, it is natural that much more energy is absorbed in that case.

On the other hand, when the impact velocity is 3 m/s, a large amount of the kinetic energy of the impactor is used for damage development and the rest is used for rebound. The same trend applies for $a/c = 0.4$. However, the absorbed energy compared to the samples with $a/c = 0.3$ remained at lower levels.

Although a clear trend was not observed in the energy graphs, more energy was absorbed in $a/c = 0.3$ samples where the surface crack width was higher due to the lower number of active laminates that provide the rigidity of the composite. Besides, almost all of this absorbed energy is used for plastic deformations. There is no significant difference between $a/c = 0.3$ and $a/c = 0.4$. However, during the production of surface cracks, relatively more regions are cut off at $a/c = 0.3$. This allows damage to be extended to a wider area and causes more energy to be emitted.

3.2 Damage progression by impact

In this section, damage formation and progression within hybrid laminated composite materials subjected to low-velocity impact were evaluated by using an optical microscope and SEM images. Figure 9 shows the optical microscope images of hybrid laminated composite materials with surface crack after impact loading. The yellow circles show the contact area where the impactor is applied, and the blue arrows indicate the damage areas on both surfaces. The fiber breakage and other permanent damage formed in the composite material are clearly visible. It is seen that severe damage formation is specially located at the surface crack tips and spread out that zone.

The damage generally starts with fiber pullout of surface crack tips and is converted to delamination. The delamination between the laminates seen in the lower parts of the

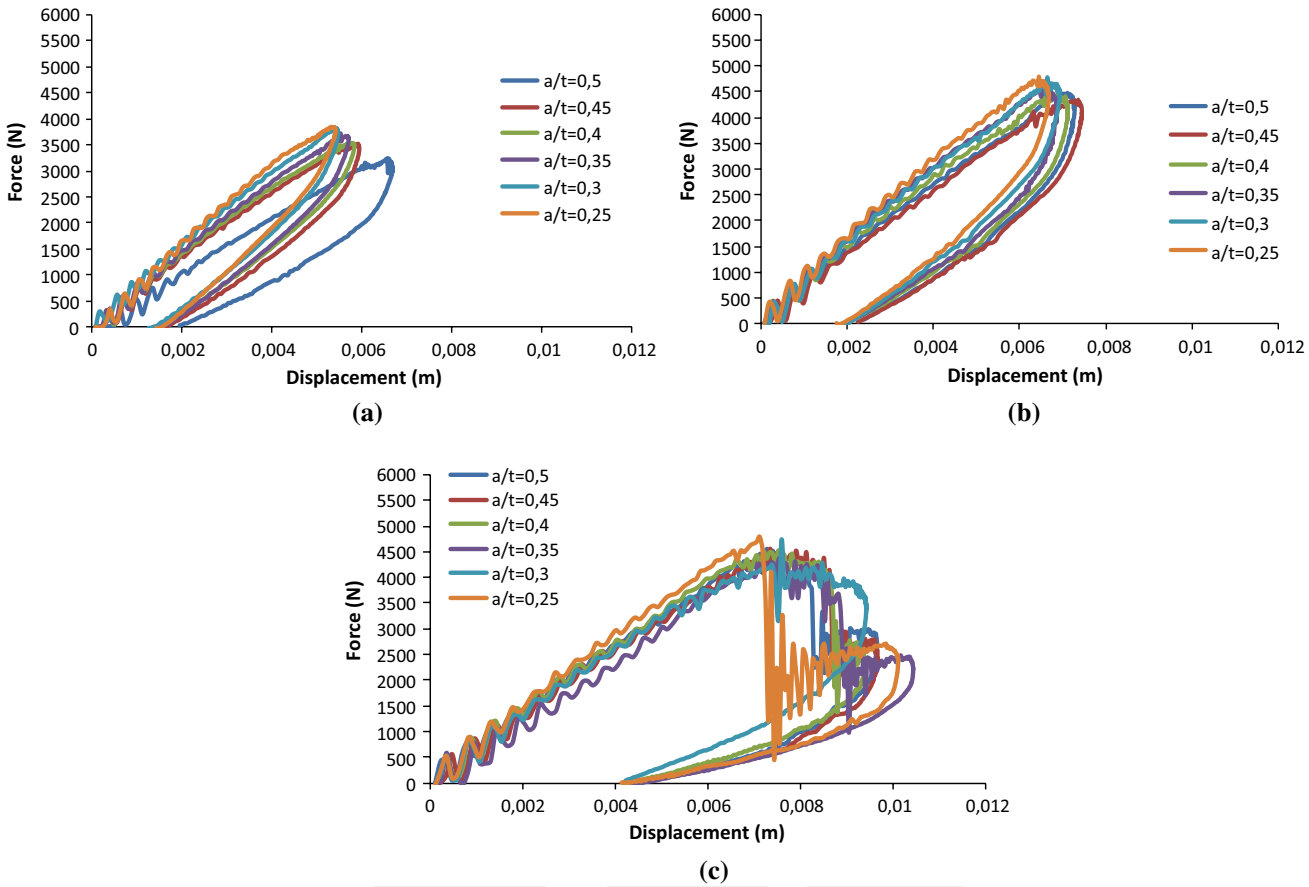

Fig. 6 Effect of different surface crack geometries on force–displacement behavior ($a/c = 0.4$)

Table 5 Change of stiffness behavior with different velocity impact

Specimen number	*a/c*	*a/t*	2 m/s		2.5 m/s		3 m/s	
			Contact stiffness (kN/s)	Bending stiffness (kN/m)	Contact stiffness (kN/s)	Bending stiffness (kN/m)	Contact stiffness (kN/s)	Bending stiffness (kN/m)
1	0.3	0.5	1234	684	1358	802	1589	610
2		0.45	1283	700	1263	739	1558	626
3		0.4	1151	643	1530	902	1534	606
4		0.35	1297	722	1494	877	1546	433
5		0.3	1390	760	1612	948	1519	629
6		0.25	1210	679	1649	951	1450	580
7	0.4	0.5	1019	562	1494	862	1526	616
8		0.45	1216	679	1466	845	1536	620
9		0.4	1258	704	1541	903	1502	622
10		0.35	1310	730	1650	964	1333	561
11		0.3	1354	760	1674	969	1579	612
12		0.25	1523	842	1744	1020	826	406

surface, as the impact velocity increases, occurs as lighter regions in Fig. 9. It is also observed that fiber buckling has also taken place on the compression side of the specimen. The fibers which are in the vicinity of the surface and are subjected to the compressive force can be easily separated from the surface by buckling. These damages occur with the energy absorbed during the impact. The ability of the fibers to carry compressive force is poor. Also, when the fibers

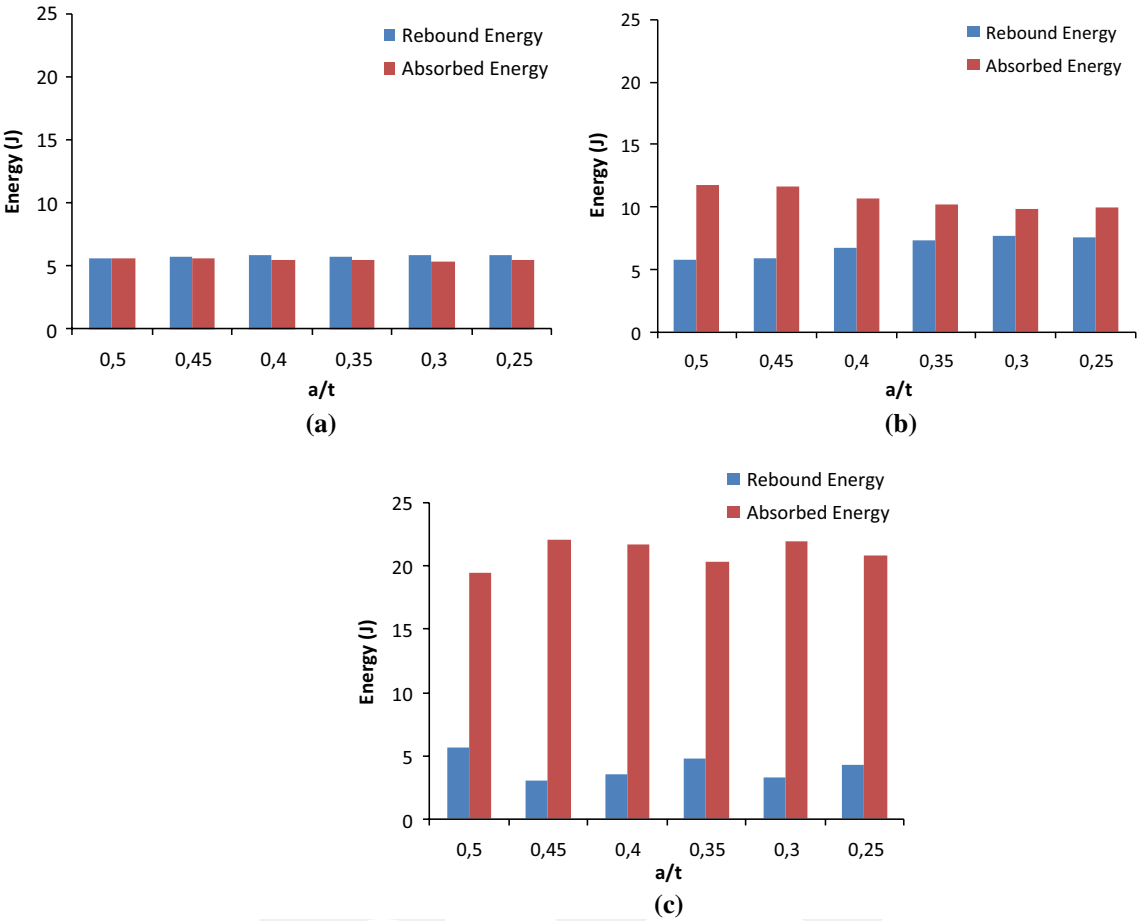

Fig. 7 Variation of energy at different impact velocities ($a/c = 0.3$). **a** 2 m/s, **b** 2.5 m/s, **c** 3 m/s

are loaded with a tensile load, the load is distributed to the environment through the matrix and a large damage area is formed. In this respect, when the tensile force is applied, the resistance is higher and the damage is spread over a wider area.

On the other hand, matrix cracking also takes place where impactor hits. Impact damage becomes more prominent as the surface crack width parameter c increases. However, the damage to the material is reduced by the reduction of the crack width. Figure 9 also shows that damage to the hybrid layered composite materials increases with increasing depth of the cracks.

In composite materials where the impact is applied at high speed (Fig. 9—3 m/s), the development of damages is seen more clearly due to the initial surface cracks with increasing energy. The elastic deformation ability is higher in the surface cracks where the width (c) is higher as seen in the force–displacement curves. Therefore, it is seen that the fibers break with the impact on the surface where the crack is exposed due to the impact force. In addition, fiber buckling is very high in the contact area of the impactor due to the bending of the composite material after impact. Depending on the increase in the absorbed energy, it is seen that the vertical direction fiber breakage marks on the impactor side are in the same direction as the surface crack. In this, it is seen that the initial surface cracks play an initiator role in the damages (matrix or fiber damages) that occur after the energy ingested.

Figure 10 shows the microstructures and damage formation of the sample tested at 3 m/s. Figure 10a shows that the damage begins with delamination that starts from the bottom of the crack and follows the tip of the machined surface crack. This formation spreads to successive laminate and appears to be partly delamination between plies. Figure 10b shows crack branching, whereas Fig. 10c shows delamination formation between the glass layers. When Fig. 10d is examined, it is seen that two parallel cracks are visible in the direction of the initial surface crack. These cracks are delamination starting from the edge of the initial surface crack and advancing toward the interior. It is also observed that deep cracks may act as delamination initiation sites. Following the shape of this elliptical surface crack is an indication that the crack passes easily from the laminate to the laminate. However, when the SEM images are examined in detail,

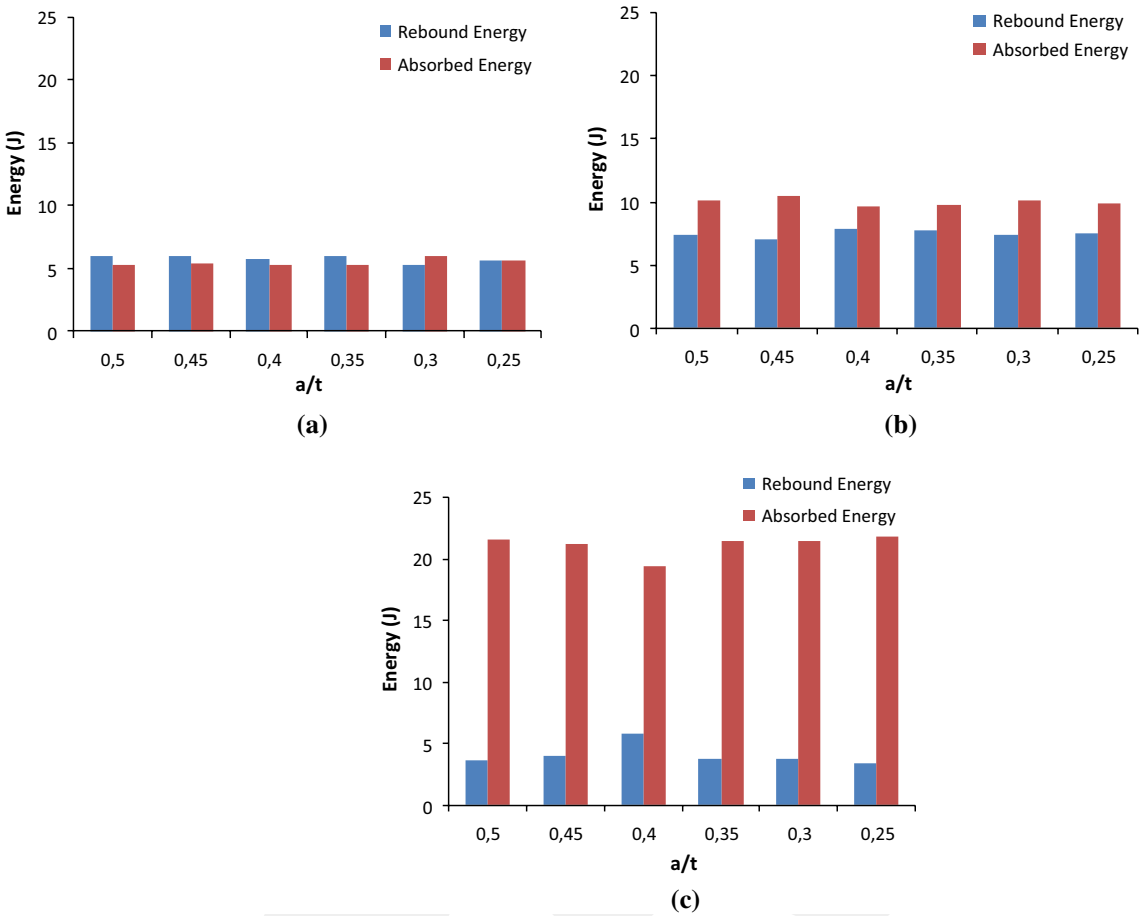

Fig. 8 Variation of energy at different impact velocities ($a/c = 0.4$). **a** 2 m/s, **b** 2.5 m/s, **c** 3 m/s

crack progression in the form of delamination appears to be easier. This is the general tendency in all samples where the microstructure is examined, and it is understood that the damage development after impact is generally in the form of delamination. Also, it is seen that there is damage development in the form of delamination in the regions far from the surface crack.

Similarly, in Fig. 10e, f, crack propagation and delamination are noticeable in the laminated composite materials due to impact load. When the materials containing different surface crack geometries are compared, it is seen that the behavior is generally similar; the initial surface crack generally triggers the delamination formation and shows itself as delamination developing around the crack. However, in the samples with $a/t = 0.25$, delamination was also found in the regions far from the initial crack. On the other hand, delamination developed in samples with $a/t = 0.5$ was observed to begin from the edge of the initial surface crack. This suggests that the stress intensity of the initiation cracks is severe enough to trigger delamination between laminates [28].

The parameters a/c and a/t influence the magnitude of the stress intensity factor. The bottom of the surface crack is usually the highest point of stress intensity factor in isotropic materials. As the a/c grows, the region with high-stress intensity expands out from the bottom of the surface crack. If the stress intensity factor is large enough, the laminates are separated. As seen in Fig. 10, crack formation proceeded at the bottom of the surface crack, followed by the surface form. However, the crack formation approached the inter-layer region after a certain progression, where the stress intensity factor was sufficiently large and the fracture was branched out.

4 Conclusions

In this study, the low-velocity impact behaviors of hybrid laminated composites with surface crack have been investigated. Surface cracks with different crack depth-to-thickness (a/t) and cracks depth-to-crack width ($a/ca/c$) ratios were machined upon hybrid laminated composites and subjected to low-velocity impact tests under 2 m/s, 2.5 m/s and 3 m/s velocities. After the low-velocity impact tests, the absorbed/rebounded energy changes were examined

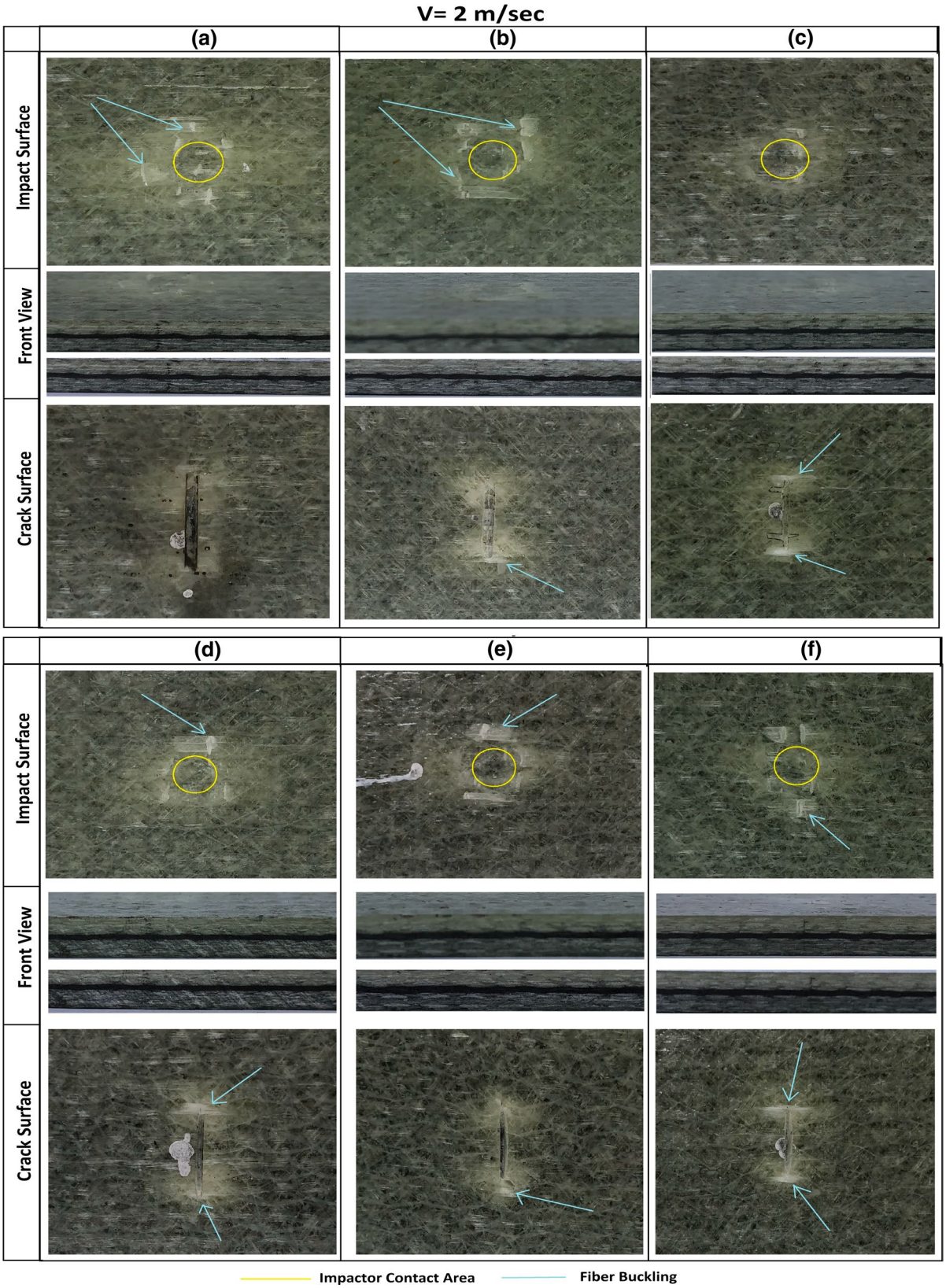

Fig. 9 Damage images of composite materials at different impact velocities **a** $a/c=0.3$ and $a/t=0.45$, **b** $a/c=0.3$ and $a/t=0.4$, **c** $a/c=0.3$ and $a/t=0.35$, **d** $a/c=0.4$ and $a/t=0.45$, **e** $a/c=0.4$ and $a/t=0.4$, **f** $a/c=0.4$ and $a/t=0.35$

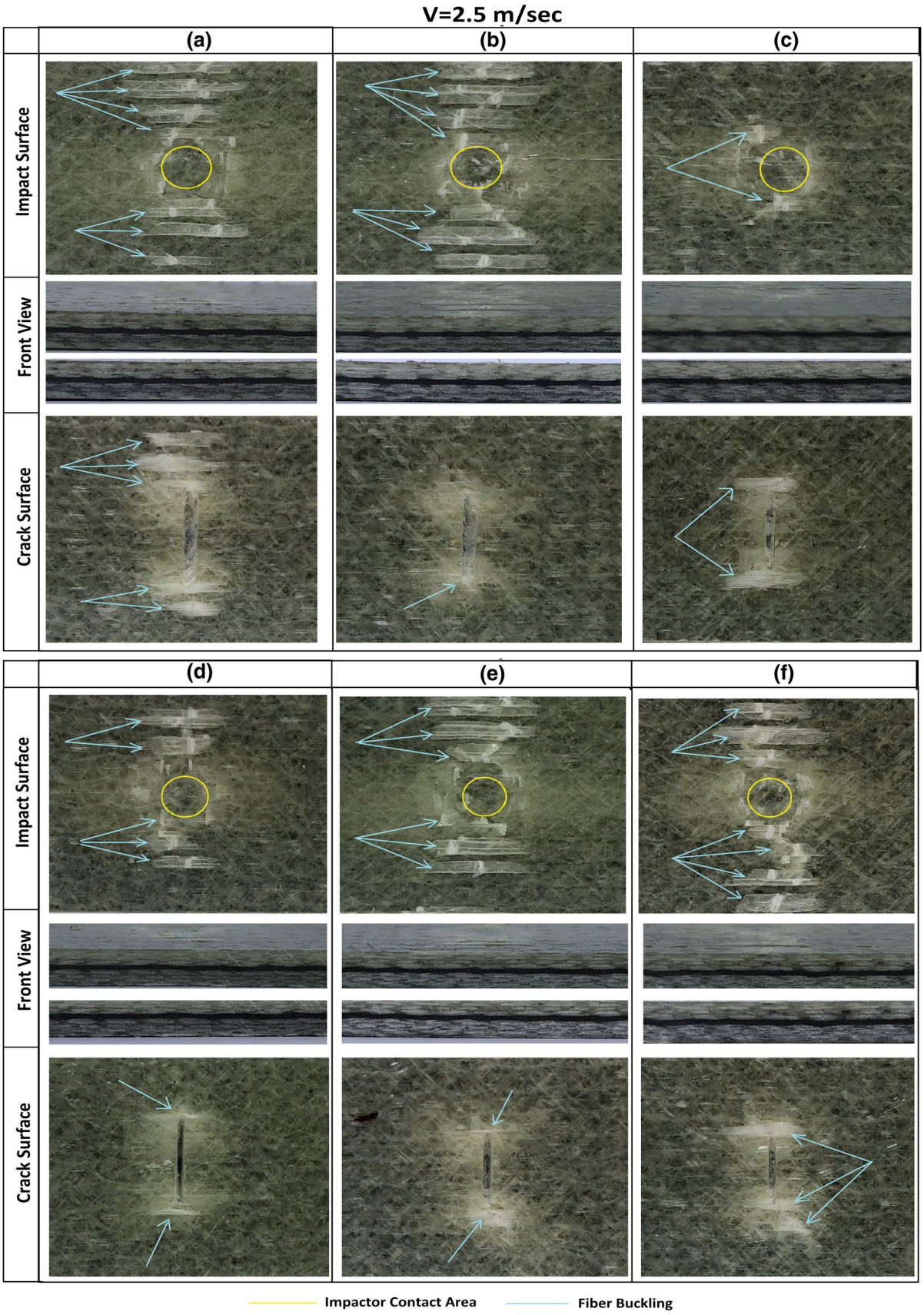

Fig. 9 (continued)

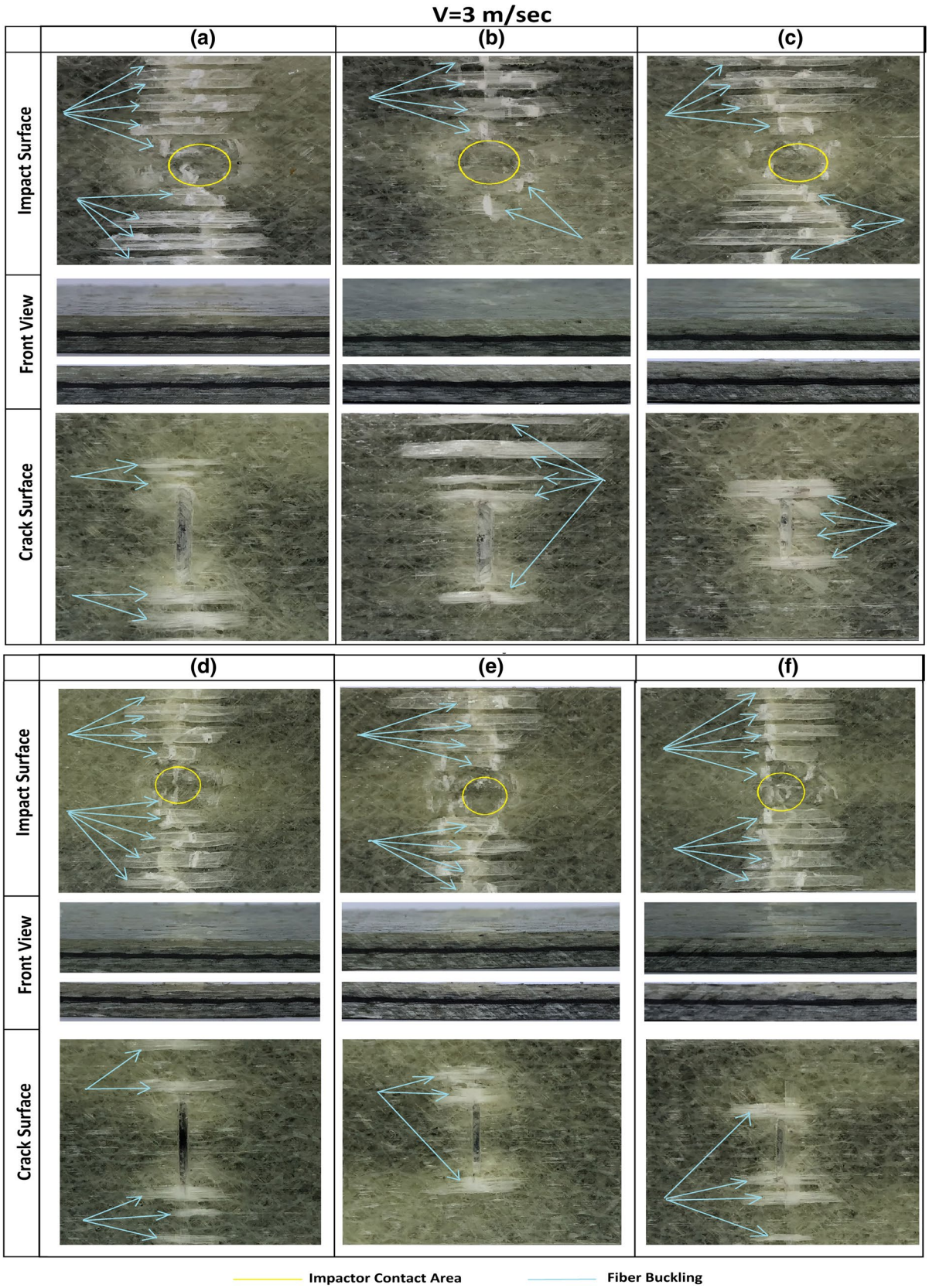

Fig. 9 (continued)

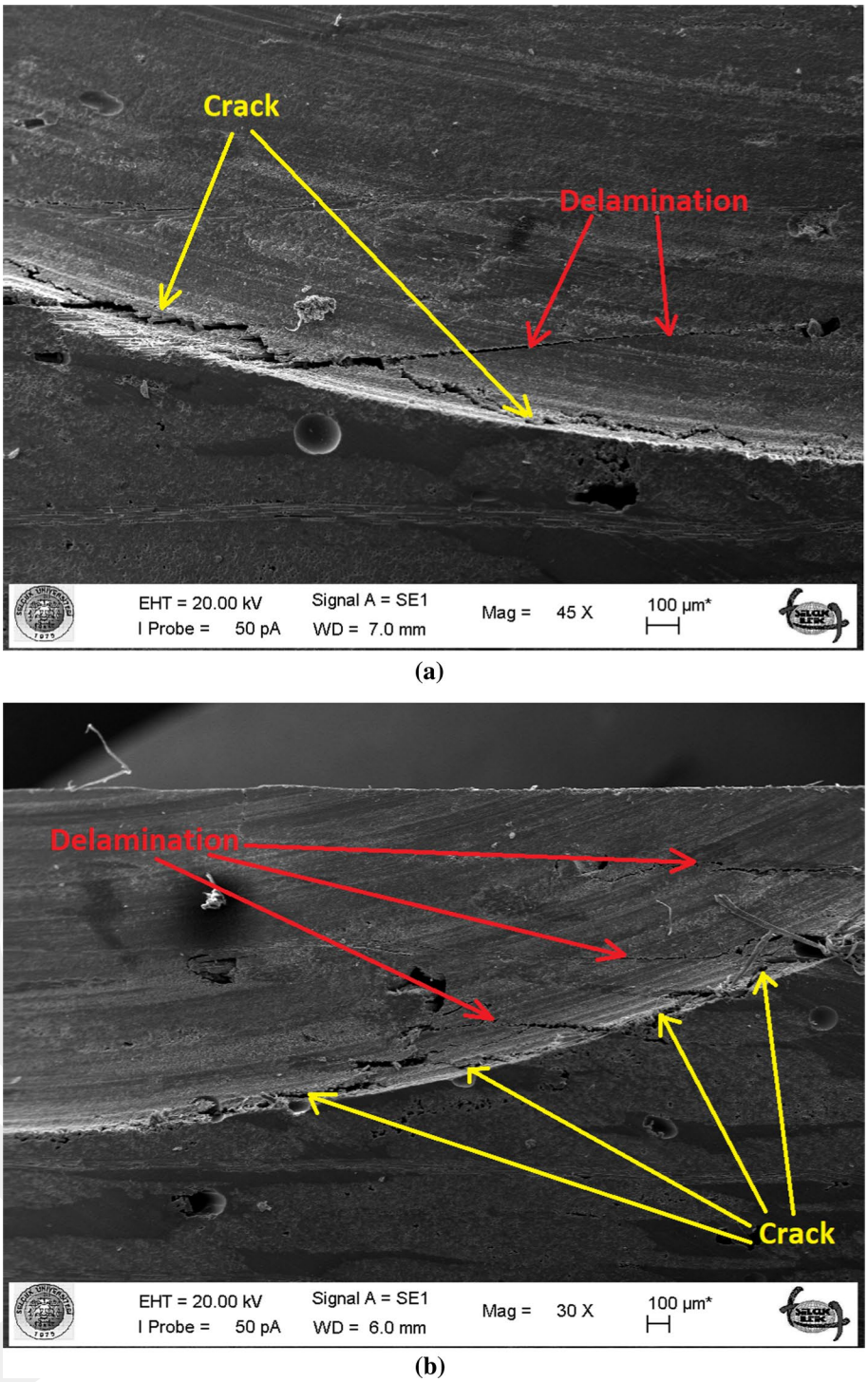

Fig. 10 SEM image of surface crack area after impact loading (3 m/s). **a** $a/c=0.3$, $a/t=0.5$, **b** $a/c=0.3$, $a/t=0.5$, **c** $a/c=0.4$, $a/t=0.5$ **d** $a/c=0.4$, $a/t=0.5$, **e** $a/c=0.3$, $a/t=0.5$, **f** $a/c=0.4$, $a/t=0.25$

along with the change of force depending on time and displacement. In addition to these evaluations, damage developments in surface cracked composite materials after impact loads were evaluated with optic microscope and SEM images. These evaluations are as follows in terms of items.

- The force value reached during the low-speed impact has decreased significantly with increasing surface crack depth (a) and surface crack width (c). For this reason, it has been determined that the surface crack affects the mechanical behavior of the composite materials and the

Fig. 10 (continued)

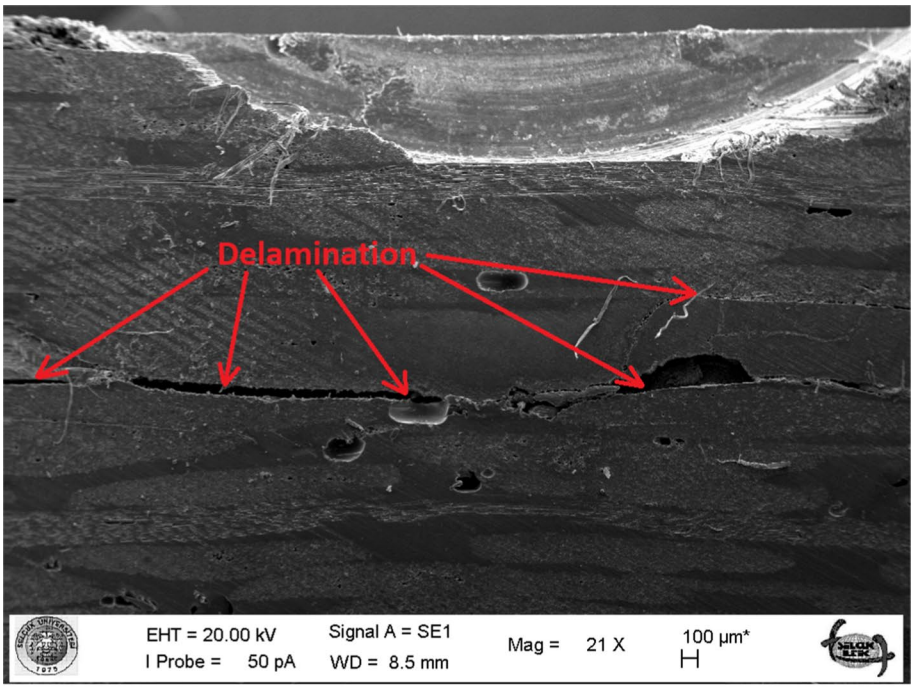

(c)

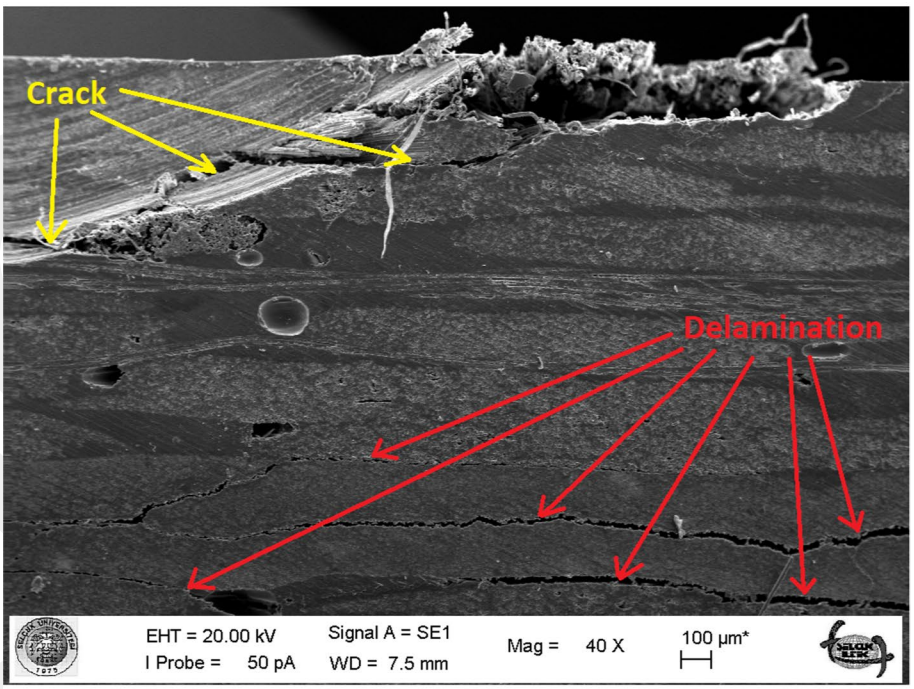

(d)

composite material stiffness decreases especially with increasing crack depth.

- Interaction time increases as the surface crack width (c) parameter of composite materials grows. This interaction time increases at 2 m/s and 2.5 m/s, but this time decreases due to the occurrence of damage mechanisms at impact velocity of 3 m/s.
- In impact tests at a velocity of 3 m/s, sudden drops in force were observed. This situation has been evaluated as the occurrence of fiber breakage and fiber pullout mechanisms as well as delaminations with the effect of increased impact force.
- The rigidity of composite materials is significantly influenced by the existing surface crack geometry. Increasing the crack depth decreases the stiffness since composite

Fig. 10 (continued)

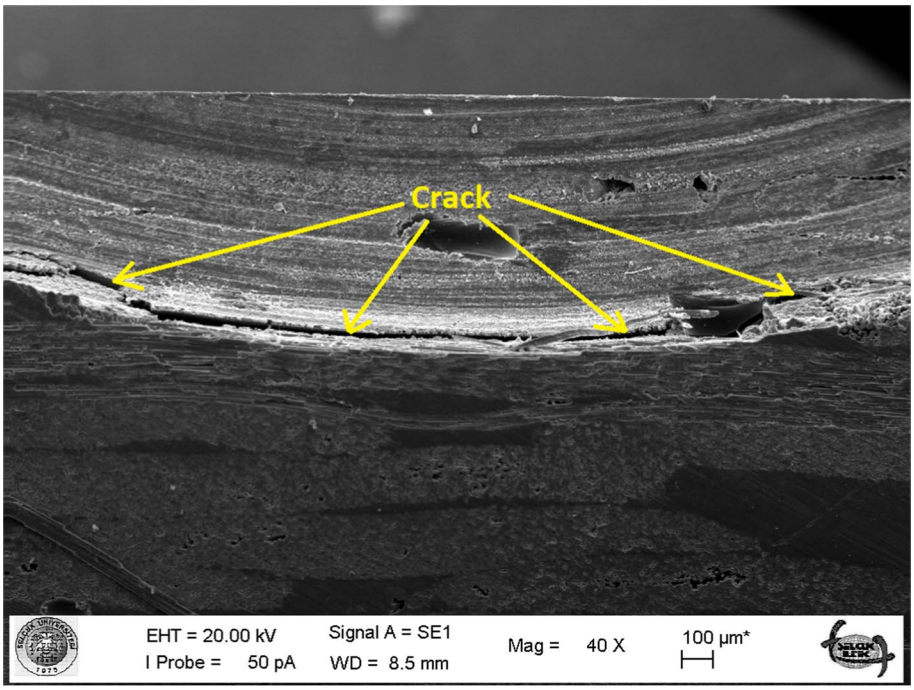

(e)

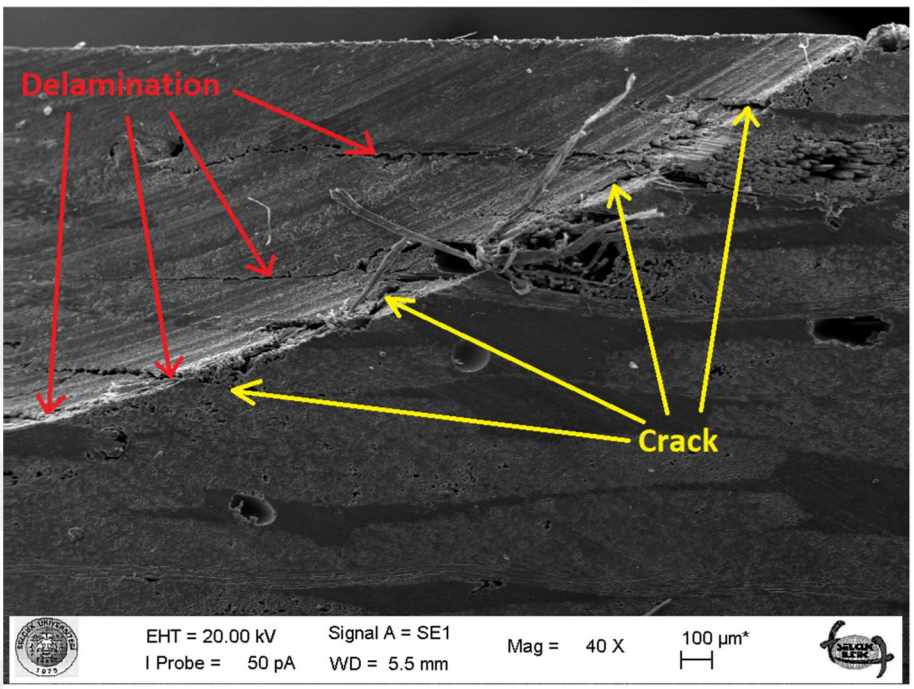

(f)

materials will reduce the number of effective laminates against dynamic effects.

- Changes in the contact and bending stiffness of composite materials due to dynamic loads are affected by the crack geometry. Elastic deformation is higher in samples with high crack width (c). However, with the increase in a/t ratio, significant decreases were observed in the stiffness. While the surface crack geometry is constant, with the increase in impact velocity, internal damage mechanisms develop and significantly increase the amount of permanent damage.
- Damage or plastic deformations occurring in composite materials after low-speed impact are related to the absorbed energy. While no significant effect was observed in energy changes at impact speeds of 2 m/s and 2.5 m/s, changes were observed due to the surface crack geometry at the

impact velocity of 3 m/s. In addition, it was observed that the amount of absorbed energy was significantly affected by the crack geometry. With the increase in the a/t ratio, the resistance of the composite material against the impact decreased and absorbed more energy. In samples with $a/c = 0.3$, the absorbed energy is partially higher. In this, as the surface crack width (c) increased, the resistance caused by friction and stiffness of each layer was effective.

- When the optical microscope images were examined, significant fiber buckling was observed depending on the compression load on the surface where the impact was applied. In addition, at 2.5 m/s and 3 m/s impact speeds, damage developments were observed on the surface where the crack was found. These damage developments caused by the increase in absorbed energy were affected by crack geometry. In the increasing crack geometry parameters, damage developments have occurred as a continuation of the surface crack.
- Looking at the SEM images, delamination was common in hybrid composite materials with surface cracks. In particular, damage to samples where the surface crack depth (a) is large is in the form of progression of the crack or the formation of new delaminations around the crack. This damage behavior becomes more evident with the increase in pulse speed.

Funding This study has been financially funded by Selçuk University (BAP) under Grant Numbers of 12401029 and 11101033.

References

1. Güneş A (2013) Investigation of dynamic behaviors of hybrid stacked composite laminates with surface crack. Ms. Thesis, Selçuk University, Department of Mechanical Engineering
2. Jin F-L, Li X, Park S-J (2015) Synthesis and application of epoxy resins: a review. J Ind Eng Chem 29:1–11
3. Kaybal HB, Ulus H, Demir O, Şahin ÖS, Avcı A (2018) Effects of alumina nanoparticles on dynamic impact responses of carbon fiber reinforced epoxy matrix nanocomposites. Eng Sci Technol Int J 21:399–407
4. Das S, Halder S, Wang J, Goyat M, Kumar AA, Fang Y (2017) Amending the thermo-mechanical response and mechanical properties of epoxy composites with silanized chopped carbon fibers. Compos A Appl Sci Manuf 102:347–356
5. Goble D, Wolff E (1993) Strain-rate sensitivity index of thermoplastics. J Mater Sci 28(22):5986–5994
6. Allaire G, Delgado G (2016) Stacking sequence and shape optimization of laminated composite plates via a level-set method. J Mech Phys Solids 97:168–196
7. Bulut M, Erklig A (2018) The investigation of quasi-static indentation effect on laminated hybrid composite plates. Mech Mater 117:225–234
8. Caminero M, García-Moreno I, Rodríguez G (2017) Damage resistance of carbon fiber reinforced epoxy laminates subjected to low velocity impact: effects of laminate thickness and ply-stacking sequence. Polym Test 63:530–541
9. Cheng X, Du X, Zhang J, Zhang J, Guo X, Bao J (2018) Effects of stacking sequence and rotation angle of patch on low velocity impact performance of scarf repaired laminates. Compos B Eng 133:78–85
10. Hosur M, Abdullah M, Jeelani S (2005) Studies on the low-velocity impact response of woven hybrid composites. Compos Struct 67(3):253–262
11. Jiang H, Ren Y, Gao B, Xiang J (2017) Numerical investigation on links between the stacking sequence and energy absorption characteristics of fabric and unidirectional composite sinusoidal plate. Compos Struct 171:382–402
12. Jing Z, Sun Q, Silberschmidt V (2016) Sequential permutation table method for optimization of stacking sequence in composite laminates. Compos Struct 141:240–252
13. Riccio A, Di Felice G, Saputo S, Scaramuzzino F (2014) Stacking sequence effects on damage onset in composite laminate subjected to low velocity impact. Procedia Eng 88:222–229
14. Sevkat E, Liaw B, Delale F, Raju B (2009) Drop-weight impact of plain-woven hybrid glass–graphite/toughened epoxy composites. Compos A Appl Sci Manuf 40(8):1090–1110
15. Sun X, Hallett S (2018) Failure mechanisms and damage evolution of laminated composites under compression after impact (CAI): experimental and numerical study. Compos A Appl Sci Manuf 104:41–59
16. Tornabene F, Fantuzzi N, Bacciocchi M, Viola E (2018) Mechanical behavior of damaged laminated composites plates and shells: higher-order shear deformation theories. Compos Struct 189:304–329
17. Vosoughi A, Darabi A, Forkhorji HD (2017) Optimum stacking sequences of thick laminated composite plates for maximizing buckling load using FE-GAs-PSO. Compos Struct 159:361–367
18. Sevkat E, Liaw B, Delale F (2013) Drop-weight impact response of hybrid composites impacted by impactor of various geometries. Mater Des 52:67–77
19. Tornabene F, Fantuzzi N, Bacciocchi M, Neves AM, Ferreira AJ (2016) MLSDQ based on RBFs for the free vibrations of laminated composite doubly-curved shells. Compos B Eng 99:30–47
20. Tornabene F, Fantuzzi N, Viola E, Ferreira A (2013) Radial basis function method applied to doubly-curved laminated composite shells and panels with a general higher-order equivalent single layer formulation. Compos B Eng 55:642–659
21. Krishnan P, Majid MA, Afendi M, Gibson A, Marzuki H (2015) Effects of winding angle on the behaviour of glass/epoxy pipes under multiaxial cyclic loading. Mater Des 88:196–206
22. Krishnan P, Majid MA, Afendi M, Yacob S, Gibson A (2016) Effects of hydrothermal ageing on the behaviour of composite tubes under multiaxial stress ratios. Compos Struct 148:1–11
23. Krishnan P, Majid MA, Yi AJ, Afendi M, Yacob S, Gibson A (2018) An automated portable multiaxial pressure test rig for qualifications of glass/epoxy composite pipes. Sci Eng Compos Mater 25(2):243–252
24. Abrate S (2005) Impact on composite structures. Cambridge University Press, Cambridge
25. Agrawal S, Singh KK, Sarkar PK (2014) Impact damage on fibre-reinforced polymer matrix composite—a review. J Compos Mater 48(3):317–332
26. Krollmanna J, Schreyer T, Veidt M, Drechsler K (2019) Impact and post-impact properties of hybrid-matrix laminates based on carbon fiber-reinforced epoxy and elastomer subjected to low-velocity impacts. Compos Struct 208:535–545
27. Jones RM (1999) Mechanics of composite materials, 2nd edn. CRC Press, Boca Raton, pp 426–453

28. Chen D, Luo Q, Meng M, Li Q, Sun G (2019) Low velocity impact behavior of interlayer hybrid composite laminates with carbon/glass/basalt fibres. Compos Part B 176:107191
29. Yang FJ, Cantwell WJ (2010) Impact damage initiation in composite materials. Compos Sci Technol 70:336–342
30. Shyr T, Pan Y (2003) Impact damage resistance and damage characteristics of composite laminates. Compos Struct 62:193–203
31. Schoeppner GA, Abrate S (2000) Delamination threshold loads for low velocity impact on composite laminates. Compos A Appl Sci Manuf 31:903–915
32. Belingardi G, Vadori R (2002) Low velocity impact tests of laminate glass-fiber-epoxy matrix composite material plates. Int J İmpact Eng 27:213–229
33. Hosur M, Abdullah M, Jeelani MS (2005) Studies on the low velocity impact response of woven hybrid composites. Compos Struct 67:253–262
34. Sutherland LS, Soares C (2007) Scaling of impact on low fiber-volume glass-polyester laminates. Compos A Appl Sci Manuf 38:307–317
35. Choi N, Chang J, Kwak S, Gu J (2010) Impact surface fractures of glass-fiber/epoxy lamina-coated glass plates by small steel-ball. Compos Sci Technol 70:2056–2062
36. Shuchang L, Xiaohu Y, Xiaoqing Z (2015) Delamination prediction in composite laminates under low-velocity impact. Compos Struct 132:290–298
37. Mili F, Necib B (2001) Impact behavior of cross-ply laminated composite plates under low velocities. Compos Struct 51:237–244
38. Zainuddin S, Arefin T, Fahim A, Hosur MV, Tyson JD, Kumar A, Trovillion J, Jeelani S (2014) Recovery and improvement in low-velocity impact properties of e-glass/epoxy composites through novel self-healing technique. Compos Struct 108:277–286
39. Güneş A, Şahin ÖS (2016) Effect of surface crack depth on hybrid laminated composites. Arch Mater Sci Eng 82(1):38–41
40. Aymerich F, Priolo P (2008) Characterization of fracture modes in stitched and unstitched cross-ply laminates subjected to low-velocity impact and compression after impact loading. Int J İmpact Eng 35:591–608
41. Avci A, Şahin ÖS, Tarakcioglu N (2007) Fatigue behavior of surface cracked filament wound pipes with high tangential strength in corrosive environment. Compos Part A Appl Sci Manuf 38:1192–1199
42. Hutař P, Ševčík M, Náhlík L, Zouhar M, Knésl Z (2014) Assessment of the stability of a surface crack in laminates. Mech Compos Mater 50:13–24
43. Riesch J, Höschen T, Linsmeier C, Wurster S, You J-H (2014) Enhanced toughness and stable crack propagation in a novel tungsten fibre-reinforced tungsten composite produced by chemical vapour infiltration. Phys Scr T159:014031
44. Mishra A, Naik NK (2010) Failure initiation in composite structures under low-velocity impact: analytical studies. Compos Struct 92:436–444
45. Li S, Reid SR, Zou Z (2006) Modelling damage of multiple delaminations and transverse matrix cracking in laminated composites due to low velocity lateral impact. Compos Sci Technol 66:827–836
46. Akdemir A, Tarakcioglu N, Avci A (2001) Stress corrosion crack growth in glass/polyester composites with surface crack. Compos B Eng 32:123–129
47. Ueda S (2002) Impact response of a piezoelectric layered composite plate with a crack. Theor Appl Fract Mech 38:221–242
48. Shin DK, Lee JJ (2001) Fracture parameters of interfacial crack of bimaterial under the impact loading. Int J Solids Struct 38:5303–5322
49. Soliman EM, Sheyka MP, Taha MR (2012) Low-velocity impact of thin woven carbon fabric composites incorporating multi-walled carbon nanotubes. Int J Impact Eng 47:39–47
50. Ulus H, Üstün T, Şahin ÖS, Karabulut SE, Eskizeybek V, Avcı A (2016) Low-velocity impact behavior of carbon fiber/epoxy multiscale hybrid nanocomposites reinforced with multi-walled carbon nanotubes and boron nitride nano plates. J Compos Mater 50(6):761–770
51. Wang H, Vu-Khanh T (1994) Damage extension in carbon fiber/PEEK crossply laminates under low velocity impact. J Compos Mater 28(8):684–707
52. Gemi L, Kara M, Avci A (2016) Low velocity impact response of prestressed functionally graded hybrid pipes. Compos Part B Eng 106:154–163
53. Cheng X, Du X, Zhang J, Zhang J, Guo X, Bao J (2018) Effects of stacking sequence and rotation angle of patch on low velocity impact performance of scarf repaired laminates. Compos Part B Eng 133:78–85
54. Kagitci YC, Tarakcioglu N (2016) The effect of weld line on tensile strength in a polymer composite part. Int J Adv Manuf Technol 85:1125–1135
55. Panettieri E, Fanteria D, Montemurro M, Froustey C (2016) Low-velocity impact tests on carbon/epoxy composite laminates: a benchmark study. Compos B 107:9–21
56. Eskizeybek V, Ulus H, Kaybal HB, Şahin ÖS, Avcı A (2018) Static and dynamic mechanical responses of $CaCO_3$ nanoparticle modified epoxy/carbon fiber nanocomposites. Compos B 140:223–231
57. Fu SY, Feng XQ, Lauke B, Mai YW (2008) Effects of particle size, particle/matrix interface adhesion and particle loading on mechanical properties of particulate–polymer composites. Compos B 39(6):933–961
58. Vaidya UK, Hosur M, Earl D, Jeelani S (2000) Impact response of integrated hollow core sandwich composite panels. Compos A Appl Sci Manuf 31(8):761–772
59. Evci C, Gülgeç M (2012) An experimental investigation on the impact response of composite materials. Int J Impact Eng 43:40–51
60. Hosur M, Mohammed A, Zainuddin S, Jeelani S (2008) Processing of nanoclay filled sandwich composites and their response to low-velocity impact loading. Compos Struct 82(1):101–116
61. Rahman M, Hosur M, Zainuddin S, Vaidya U, Tauhid A, Kumar A et al (2013) Effects of amino-functionalized MWCNTs on ballistic impact performance of Eglass/epoxy composites using a spherical projectile. Int J Impact Eng 57:108–118
62. Rahman M, Zainuddin S, Hosur M, Malone J, Salam M, Kumar A et al (2012) Improvements in mechanical and thermo-mechanical properties of e-glass/epoxy composites using amino functionalized MWCNTs. Compos Struct 94(8):2397–2406
63. Cho WS, Cho MW, Lee JH, Munir ZA (2006) Effects of h-BN additive on the microstructure and mechanical properties of AlN-based machinable ceramics. Mater Sci Eng 418(1):61–67
64. Rahman MM, Hosur M, Hsiao KT, Wallace L, Jeelani S (2015) Low velocity impact properties of carbon nanofibers integrated carbon fiber/epoxy hybrid composites manufactured by OOA–VBO process. Compos Struct 120:32–40
65. Gemi L, Şahin ÖS, Akdemir A (2017) Experimental investigation of fatigue damage formation of hybrid pipes subjected to impact loading under internal pre-stress. Compos Part B Eng 119:196–205
66. Abrate S (1991) Impact on laminated composite materials. Appl Mech Rev 44(4):155–190
67. Gemi L, Kayrıcı M, Uludağ M, Gemi DS, Şahin ÖS (2018) Experimental and statistical analysis of low velocity impact response of filament wound composite pipes. Compos B 149:38–48
68. Farley GL (1987) Energy absorption in composite materials for crashworthy structures. In: 6th international conference on composite materials, July 20, 1987–July 24, 1987, London, United Kingdom

69. Farley GL (1991) The effects of crushing speed on the energy-absorption capability of composite tubes. J Compos Mater 25(10):1314–1329
70. Mamalis A, Manolakos D, Ioannidis M, Papapostolou D (2005) On the response of thinwalled CFRP composite tubular components subjected to static and dynamic axial compressive loading: experimental. Compos Struct 69(4):407–420